

EFFECTS OF SOIL MOISTURE HETEROGENEITY ON BOUNDARY LAYER FLOW WITH COUPLED GROUNDWATER, LAND-SURFACE, AND MESOSCALE ATMOSPHERIC MODELING

Fotini Katopodes Chow^{1*}, Stefan J. Kollet², Reed M. Maxwell², and Qingyun Duan²

¹Department of Civil and Environmental Engineering, University of California, Berkeley, California

²Atmospheric, Earth, and Energy Department, Lawrence Livermore National Laboratory, Livermore, California

1. Introduction and background

Mesoscale atmospheric models currently rely on an integrated land-surface model to provide fluxes of heat, momentum, and moisture from the land surface to the atmosphere. While improvements have been made by tuning land-surface models for a variety of test cases, current models are limited to vertical transport in a shallow soil column. They are thus unable to capture lateral transport of soil moisture and limited in their ability to provide spatial variability in predicted land surface fluxes. Current mesoscale atmospheric models are therefore not provided with realistic fluxes at the surface because land-use models cannot represent runoff and subsurface lateral transport that is present when terrain or moisture gradients exist. This can lead to errors in model predictions during periods when thermal forcing dominates the diurnal development of the boundary layer.

Starting with a so-called leaky-bucket parameterization (Manabe et al. 1965), climate models have steadily evolved to use a more sophisticated lower boundary condition into what is commonly known as the land surface model (LSM). LSMs play an important role in determining fluxes from the land surface to the atmospheric boundary layer (see e.g. the review by Betts et al. 1996). A large number of LSMs have been developed, with differing parameterizations and levels of sophistication. This led to a number of inter-comparison studies, the Project for Intercomparison of Land-Surface Parameterization Schemes (PILPS), for a range of climatic conditions (Henderson-Sellers and Henderson-Sellers 1995; Shao and Henderson-Sellers 1996; Chen and Coauthors 1997; Qu and Coauthors 1998; Lohmann and Coauthors 1998; Pitman and Coauthors 1999; Schlosser and Coauthors 2000; Luo et al. 2003). As LSMs ignore the deeper soil moisture processes and the saturated zone (i.e. groundwater), there has been recent interest in incorporating a groundwater component into LSMs (Liang et al. 2003; Maxwell and Miller 2005; Yeh and Eltahir 2005). While LSMs have grown in sophistication, until this current study, lateral subsurface and overland flow have not been explicitly accounted for.

The focus of this work is to understand the influence of soil moisture variability on atmospheric boundary layer forcing. To gain this understanding requires the development of a three-dimensional, fully-coupled groundwater-atmospheric flow model, as described in this work. That soil moisture and temperature variability affects atmospheric boundary layer development has been shown through previous studies. Chow et al. (2006) found that soil moisture initialization was a crucial factor in accurate simulations of thermally-forced valley wind systems in the Swiss Alps using the ARPS mesoscale model. An off-line hydrologic model was used to provide improved spatial variability to the soil moisture in the valley, significantly improving prediction of wind transitions in the valley. Desai et al. (2005) examined the effect of improved soil moisture data and land-surface physics representations on simulations of the atmospheric boundary layer during July 1997 (SGP97), with mixed results in the extent of the influence on dry sunny days. York et al. (2002) investigated the effects of a single-column atmospheric model connected to a single layer ModFlow-based groundwater model through a reservoir-type land surface scheme. They investigated a small watershed in Kansas and found an effect of aquifer levels on evapotranspiration.

Despite previous work in this area, determining the effect of land-surface heterogeneity on the development of the atmospheric boundary layer remains unresolved. Is the effect of land-surface heterogeneity reflected in atmospheric heterogeneity? On what time scales is the effect of soil moisture variations felt in the atmosphere? How do land-surface changes affect local precipitation events? How can we best represent these processes for numerical simulations of atmospheric flow and transport over a watershed, and eventually over a larger region?

To address these questions and others, this paper describes the development of a 3D variably-saturated groundwater flow model with surface runoff capabilities dynamically coupled within a mesoscale atmospheric model to investigate the effects of soil moisture heterogeneity on boundary layer processes. In particular, we have coupled ParFlow, a 3D parallel unsaturated/saturated groundwater flow model (Ashby and Falgout 1996; Jones and Woodward 2001), with the Advanced Regional Prediction System (ARPS), a mesoscale atmospheric model (Xue et al. 2000, 2001). ParFlow also includes a fully-coupled overland flow or runoff component (Kollet and Maxwell 2006), and thus provides ARPS with soil moisture information that in-

*Corresponding author address: Department of Civil and Environmental Engineering, University of California, Berkeley, MC 1710, Berkeley, CA 94720-1710, email: chow@ce.berkeley.edu

cludes the effects of ponding, runoff, and seepage. In turn, ARPS, through its land-surface model, provides ParFlow with precipitation and evapotranspiration inputs. This leads to a fully coupled model which can represent spatial variations in land-surface forcing driven by 3D atmospheric and subsurface components.

Our test case is the Little Washita watershed in Oklahoma, which has been the subject of numerous studies and provides a unique source of subsurface, surface, and atmospheric data for validation. Here we report on the coupling procedure and preliminary simulation results for the coupled groundwater/land-surface/atmospheric model.

2. Little Washita watershed, SGP99

The Little Washita watershed is located in central Oklahoma and has been the focus of several studies (e.g. Jackson et al. 1999; Vine et al. 2001; Guha et al. 2003), with the result that it is the source of an extensive observational dataset. We focus on the data from the Southern Great Plains (SGP) experiment of 1999, from which there are special remote sensing observations of soil moisture available to complement standard time series available at surface stations scattered throughout the area. Figure 1 shows a map of the watershed and the locations of selected observation sites. The ARS Micronet stations shown on this figure are a surface network which collects rainfall, air and soil temperature at 5-15 minute intervals. Also important are measurements of streamflow in the Little Washita river (at locations shown in Figure 1) as well as groundwater table elevation measurements. The Little Washita watershed thus provides a unique dataset for validation of our coupled groundwater, land-surface, and atmospheric model.

3. Model components

We begin with a description of the individual model components for the atmospheric boundary layer, the land surface, and the subsurface.

a. Atmospheric model

As the focus of this work is on regional and local atmospheric dynamics, ARPS is used as the mesoscale atmospheric model. ARPS was developed at the Center for Analysis and Prediction of Storms at the University of Oklahoma, and is formulated as a large-eddy simulation (LES) code that solves the three-dimensional, compressible, non-hydrostatic, filtered Navier-Stokes equations. ARPS is described in detail by Xue et al. (2000, 2001).

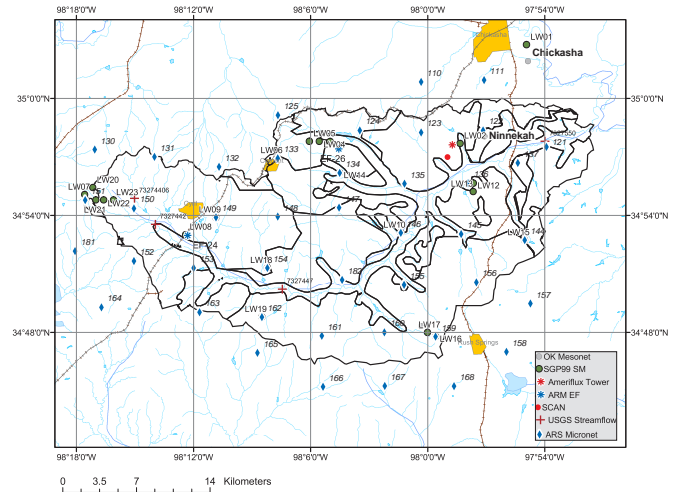


Figure 1: Little Washita watershed (black outline) and observation stations.

Fourth-order spatial differencing is used for the advection terms. Temporal discretization is performed using a mode-splitting technique to accommodate high-frequency acoustic waves. The large time steps (Δt) use the leapfrog method; first-order forward-backward explicit time stepping is used for the small time steps ($\Delta \tau$), except for terms responsible for vertical acoustic propagation, which are treated semi-implicitly. Lateral boundary conditions and initial conditions are provided from the NOAA North American Regional Reanalysis (NARR) dataset, available at 32 km resolution and at three-hourly intervals. Multiple resolutions (9 km, 3 km, 1 km, and ultimately 350 m horizontal grid spacings) are used to nest down from the NARR forcing to the domain that encompasses the Little Washita.

b. Land-surface models

The characteristics of the land surface determine sensible and latent heat flux exchange with the atmosphere. The ARPS land-surface soil-vegetation model solves surface energy and moisture budget equations, described in detail in Xue et al. (2001); Ren and Xue (2004). ARPS generally uses 13 soil types (including water and ice), and 14 vegetation classes (following the United States Department of Agriculture classifications). Land use, vegetation, and soil type data for the 1 km and coarser grids are obtained from USGS 30 second global data.

For the soil temperature and moisture budgets, two soil layers of depths 0.01 m and 1.0 m for the surface and deep soil are used. In the standard procedure, soil temperature and moisture for all grids are initialized using values interpolated from the NARR dataset. The soil moisture and temperature values at 9 km resolution are then interpolated to the 3 km resolution grid and finer grids.

For the coupled simulations, high-resolution soil moisture initialization data were obtained from ParFlow-CLM (PF.CLM), described further below, to represent the spatial variability in the Little Washita watershed better. PF.CLM is driven by NARR meteorological data and provides soil moisture data at the 1 km and 350 m grid levels for ARPS.

c. Ground water model: ParFlow

ParFlow is a parallel, variably saturated groundwater flow simulator, and is described in detail by Ashby and Falgout (1996) and Jones and Woodward (2001). In the mode employed here, it solves the Richards equation in three dimensions using a parallel, globalized Newton method. ParFlow has been modified to include the Common Land Model (CLM) (Dai et al. 2003), as described in Maxwell and Miller (2005), as well as an integrated overland flow simulator (Kollet and Maxwell 2006), which solves the shallow water equations. ParFlow has the unique capability to explicitly resolve streamflow without the use of parameterized river routing subroutines. During model spinup, overland flow naturally develops in the appropriate topographic depressions that define the river corridors, which are resolved by the model. For the groundwater flow solution, ParFlow employs an implicit backward Euler scheme in time, and a cell-centered finite difference scheme in space. At the cell interfaces, the harmonic averages of the saturated hydraulic conductivities and a one-point upstream weighting of the relative permeabilities are used. For the overland flow component, ParFlow uses an upwind finite-volume scheme in space and an implicit backward Euler scheme in time.

The input data required by ParFlow consists of the subsurface hydraulic properties, such as the saturated hydraulic conductivity K_s , porosity, ϕ , and the van Genuchten parameters for the pressure-saturation relationships. The hydraulic properties of the deeper subsurface were derived as average values from some 200 borehole logs collected in the region. 390 grid points are used in the vertical with 0.5 m resolution. The land surface cuts through the computational domain, giving variable numbers of grid points in the subsurface, as shown in Figure 2. The maximum depth of the aquifer below the subsurface is approximately 190 m, with a no-flow boundary condition at the bottom of the computational domain. The maximum depth value was chosen from borehole information and results from other studies in that region (e.g. Davis 1955) and facilitates modeling of deep groundwater flow. The regionally uniform porosity value of $\phi = 0.4$ [-] corresponds to the arithmetic average. The average value of for K_s was set to be $10m/day$ initially, but was adjusted during the spinup to better match the measured hydrographs along the Little Washita River. The calibrated value is $K_s = 5m/day$, which is about a factor of five larger than the arithmetic mean from the borehole information. We explain this discrepancy with the quite limited and un-

certain information obtained from the borehole logs and the smoothed topography at 1 km resolution, which results in generally smoother water table relief and thus smaller gradients.

The van Genuchten parameters correspond to a sandy loam, which we consider a representative value for the watershed at this point in our study. The top two 0.5-m thick layers in ParFlow extending to 1 m depth below the ground surface are considered topsoil. The soil information including the aforementioned hydraulic properties was derived from the soil cover information used by ARPS and the results of a study by Schaap and Leij (1998). In this study, the soils considered in spatially distributed fashion are sand, sandy loam, silt loam, loam, and clay loam. Topographic slopes were derived from the digital elevation model after filling sinks (areas of local convergence in the topography) by locally smoothing the topography. The Manning's coefficient used in the overland flow simulator is applied uniformly in space, though it can be distributed to reflect non-uniform surface roughness in the future.

Model spinup was required to generate realistic soil moisture distributions. This was performed offline using atmospheric forcing provided by the NARR reanalysis dataset. For this spinup the land surface model CLM was used (the fully coupled simulations described below use the ARPS LSM). After repeated application of forcing from September 1998 to October 1999, the simulation results were compared to measured time series (not shown). These included hydrographs, soil moisture curves from the SCAN site, and temperature curves from the Micronet station network. No comprehensive calibration was performed.

4. Fully-coupled groundwater-land-atmosphere simulations

The coupled PF.ARPS is applied to the Little Washita watershed and the simulation is advanced for 48 hours starting at 0 UTC on July 8, 1999. This time period was chosen because of the density of field measurements available for soil moisture conditions as well as the presence of rain events. Preliminary results from simulations with 1 km resolution and 48×35 grid points in the horizontal are described below. PF.ARPS uses 53 grid levels in the atmosphere for these simulations, with 40 m spacing near the ground and stretched above to give an average spacing of 400 m over the 20 km domain height. The subsurface component uses 390 levels with constant 0.5 m spacing in the vertical for a subsurface depth of 195 m. Lateral boundary conditions for PF.ARPS are provided by the 3 km (horizontal resolution) ARPS simulations covering a larger domain.

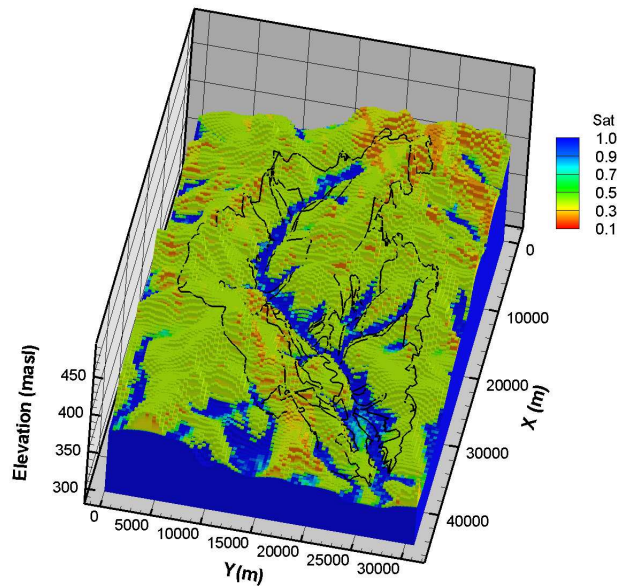


Figure 2: Soil moisture field from 350m resolution offline ParFlow simulation after spinup. Soil moisture concentrations (blue is saturated, red is 10% saturated) are shown on the topographic relief surface.

a. Coupling approach

The fully coupled simulations require the simultaneous solution of 3D groundwater flow and 3D atmospheric flow processes, with the land surface model at the interface to pass surface momentum, moisture, and heat fluxes between the models. The coupling has been performed by adding ARPS as a subroutine to ParFlow. The land-surface model is provided by the two-layer force-restore method within ARPS. The general solution procedure begins with the explicit advancement of ARPS for one hour using an internal timestep of 1 second. Surface fluxes that are relevant to ParFlow, such as infiltration and evaporation rates are integrated over the entire hour and used to provide surface fluxes at the new time for implicit time advancement of ParFlow that uses an internal 1-hour timestep. The subsurface moisture field calculated by ParFlow is passed to the land-surface model within ARPS by simply circumventing the original water balance calculations. This soil moisture information is then used by the land surface model in ARPS in the next time step. Note that for each internal ARPS time step of one second the land-surface model is also advanced, without changes in the soil moisture, which is now calculated in ParFlow. This approach may lead to small errors during rainfall events or quick drying periods. However, preliminary investigation determined that these errors are small especially when compared to the influence of differences in ParFlow vs a single-column soil model. A comprehensive analysis of this

error will be performed in the future.

b. Surface initialization

Land use data, including soil and vegetation types, are obtained from the STATSGO USGS database at 1 km resolution. Land surface elevation data from USGS are given at 3 arc second intervals. The fully coupled PF.ARPS simulations use initial soil moisture fields provided by the spun-up PF.CLM model for the appropriate date and time. The two-layer soil moisture variables in the land-surface component of ARPS are thus overwritten by moisture fields provided by PF.CLM. Initial soil temperature is provided by interpolated fields from the NARR data set and equilibrates to the PF.CLM values in approximately 24 hours of coupled simulation time.

c. Soil moisture and temperature fields

Figure 3 shows the soil moisture and temperature fields from PF.ARPS compared with those from the uncoupled ARPS simulation after 24 hours. It is immediately evident that large differences exist. The PF.ARPS soil moisture field shows the distinct signature of the Little Washita River, with much wetter conditions along the river corridor and drier conditions in the uplands. This is due to the convergence of deeper groundwater water flow at discharge zones that are the Little Washita River valley and its tributaries. Additional variability is a result of the influence of the distributed soil and vegetation cover, which is, however, much less pronounced than the impact of the topography. In contrast, the uncoupled ARPS soil moisture field shows very small spatial variability, due to the inability of the model to account for topographically-induced lateral groundwater flow. Because of the nature of the land-surface model in ARPS, the soil moisture values at a given grid cell can only be affected by shallow soil properties at that x, y location, the land cover, and the atmospheric conditions, which are of minor influence during the short simulation period.

Large differences exist also for the soil temperature fields, with PF.ARPS showing lower soil temperatures along the river corridor as a result of wetter soils. The uncoupled ARPS results lack the distinct spatial variability associated with the topography. Any spatial variability in the ARPS simulation is a result of variability in surface soil type and variability in atmospheric and solar processes (e.g. radiation, air temperature). In parts of the uplands PF.ARPS also arrives at much larger temperature values, which correspond to the drier conditions along the ridges and hill tops.

d. Surface wind and temperatures

The effect of these large soil moisture differences on the atmospheric boundary layer evolution becomes apparent in the coupled PF.ARPS simulations. Figure 4 shows the potential temperature at the surface for both the coupled and uncoupled simulations. The potential

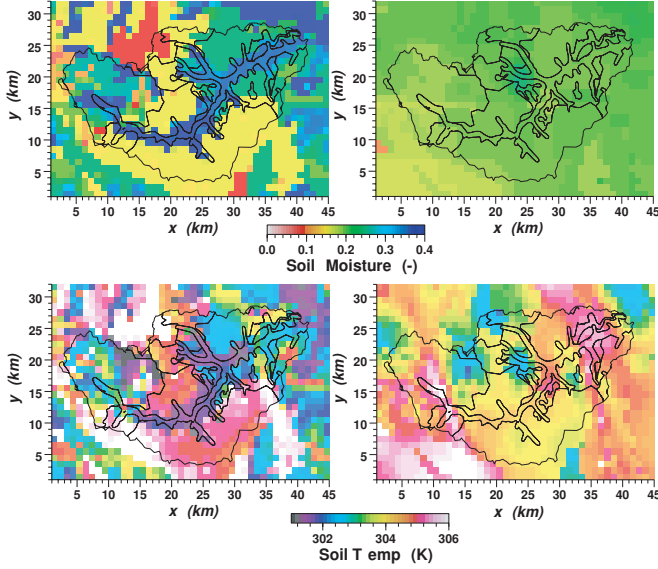


Figure 3: Comparison of soil moisture (upper) and temperature (lower) fields for PF.ARPS (left) and ARPS (right).

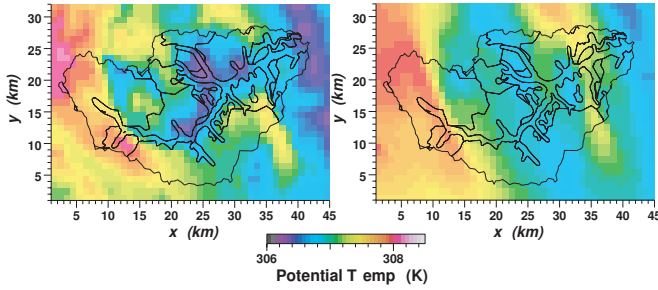


Figure 4: Comparison of potential temperature field for PF.ARPS (left) and ARPS (right) at the first model level above the ground.

temperature for PF.ARPS shows effects of the PF.ARPS soil moisture and temperature fields, with cooler air temperatures along the cooler and wetter river valley areas.

Figure 5 shows the differences in the the u and v component of the wind speed. The differences are calculated as the $u_{ARPS} - u_{PF.ARPS}$ and $v_{ARPS} - v_{PF.ARPS}$. A general increase in the v components is observed in the river valley, where the temperature is lower and the soil moisture is higher in PF.ARPS compared to the uncoupled ARPS control run. The v velocity components decrease along the topographic ridges and hilltops, where the temperatures are the largest. This trend is reversed for the u -component, which appears to be generally increasing in the valley and decreasing along the topographic ridges and hilltops.

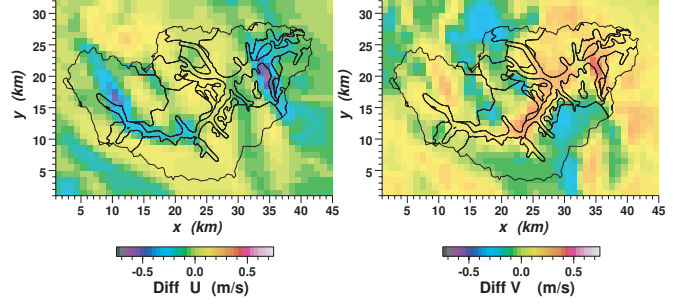


Figure 5: Difference in PF.ARPS ARPS for the U (left) and V (right) velocity components at the first model level above the ground.

5. Discussion and future work

Figures 3-5 show significant differences in the coupled and uncoupled simulations at the ground surface caused by differences in soil moisture and temperature. Vertical profiles (not shown) indicate differences in meteorological variables predominantly in the near-surface region, with the uncoupled and coupled simulations giving nearly identical results aloft. This is not surprising given that the differences in the coupled and uncoupled simulations are provided through the surface forcing. Furthermore, the current computational domain is too small to allow for adequate development of boundary layer features without excessive influence from the lateral boundary conditions. Results from higher-resolution (350 m) simulations and from longer time periods will be reported on in the near future.

An interesting observation, however, is the increased sensitivity of the atmospheric development to surface conditions preceding rain events. Because of the large differences in soil moisture, local precipitation events develop quite differently in ARPS vs PF.ARPS. We have observed localized differences on the order of 10% in accumulated precipitation (not shown). Further investigation of such precipitation events is in progress. In addition, future work will include coupled simulations at higher resolution and over larger horizontal domain sizes to minimize the effect of the lateral boundary conditions. The preliminary observations reported here indicate the potential for improved predictions of boundary layer processes given the sensitivity to surface moisture and temperature conditions during thermally forced boundary layer development and the improved ability to represent spatial variability in surface forcing using our coupled modeling approach. Ultimately our approach will be applied to much larger domains to investigate the effect on regional climate predictions on seasonal time scales. Incorporation of lateral moisture transport through subsurface flow will be of particular importance on these larger time scales; current atmospheric and land-surface models are unable to capture these processes.

Acknowledgement This work was conducted under the auspices of the U. S. Department of Energy by the University of California, Lawrence Livermore National Laboratory (LLNL) under contract W-7405-Eng and was funded by the LLNL LDRD program.

References

- Ashby, S. F. and R. D. Falgout, 1996: A parallel multigrid preconditioned conjugate gradient algorithm for groundwater flow simulations. *Nuclear Science and Engineering*, **124**, 145–159.
- Betts, A., J. Ball, A. Belijaar, M. Miller, and P. Viterbo, 1996: The land surface-atmosphere interaction: A review based on observational and global modeling perspectives. *Journal of Geophysical Research*, **101**, 7209–7225.
- Chen, T. and Coauthors, 1997: Cabauw experimental results from the project for intercomparison of land-surface parameterization schemes. *Journal of Climate*, **10**, 1194–1215.
- Chow, F. K., A. P. Weigel, R. L. Street, M. W. Rotach, and M. Xue, 2006: High-resolution large-eddy simulations of flow in a steep Alpine valley. Part I: Methodology, verification, and sensitivity studies. *Journal of Applied Meteorology and Climatology*, **45**, 63–86.
- Dai, Y., X. Zeng, R. Dickinson, I. Baker, G. Bonan, M. Bosilovich, A. Denning, P. Dirmeyer, P. Houser, G. Niu, K. Oleson, C. Schlosser, and Z. Yang, 2003: The common land model. *Bulletin of the American Meteorological Society*, **84**, 1013–1023.
- Davis, L. V., 1955: Geology and ground water resources of frady and nothern stephens counties, Oklahoma. Bulletin no. 73, Oklahoma Geological Survey.
- Desai, A. R., K. J. Davis, C. J. Senff, S. Imail, E. Browell, D. R. Stauffer, and B. P. Reen, 2005: A case study on the effects of heterogeneous soil moisture on mesoscale boundary-layer structure in the Southern Great Plains, U.S.A. Part I: simple prognostic model. *Boundary-Layer Meteorology*, **119**, doi:10.1007/s10546-005-9024-6.
- Guha, A., J. M. Jacobs, T. J. Jackson, M. H. Cosh, E.-C. Hsu, and J. Judge, 2003: Soil moisture mapping using ESTAR under dry conditions from the Southern Great Plains experiment (SGP99). *IEEE Transactions on Geoscience And Remote Sensing*, **41**, 2392–2397.
- Henderson-Sellers, A. and B. Henderson-Sellers, 1995: Simulating the diurnal temperature range: Results from phase 1(a) of the project for intercomparison of landsurface parameterisation schemes (PILPS). *Atmospheric Research*, **37**, 229–248.
- Jackson, T. J., D. M. L. Vine, A. Y. Hsu, A. Oldak, P. Starks, C. T. Swift, J. D. Isham, and M. Haken, 1999: Soil moisture mapping at regional scales using microwave radiometry: The Southern Great Plains Hydrology Experiment. *IEEE Transactions on Geoscience And Remote Sensing*, **37**, 2136–2151.
- Jones, J. E. and C. S. Woodward, 2001: Integrated surface-groundwater flow modeling: a free-surface overland flow boundary condition in a parallel groundwater flow model. *Advances in Water Resources*, **24**, 763–774.
- Kollet, S. J. and R. M. Maxwell, 2006: Integrated surface-groundwater flow modeling: a free-surface overland flow boundary condition in a parallel groundwater flow model. *Advances in Water Resources*, **in press**.
- Liang, X., Z. Xie, and M. Huang, 2003: A new parameterization for surface and groundwater interactions and its impact on water budgets with the variable infiltration capacity (VIC) land surface model. *Journal of Geophysical Research*, **108**, 4125.
- Lohmann, D. and Coauthors, 1998: The project for intercomparison of land-surface parameterization schemes PILPS phase 2(c) - Red Arkansas River basin experiment: 3. spatial and temporal analysis of water fluxes. *Global and Planetary Change*, **19**, 161–179.
- Luo, L., , and Coauthors, 2003: Effects of frozen soil on soil temperature, spring infiltration, and runoff: Results from the PILPS 2(d) experiment at Valdai, Russia. *Journal of Hydrometeorology*, **4**, 334–351.
- Manabe, S., J. Smagorinsky, and R. Strickler, 1965: Simulated climatology of a general circulation model with a hydrologic cycle. *Monthly Weather Review*, **93**, 769–798.
- Maxwell, R. and N. Miller, 2005: Development of a coupled land surface and groundwater model. *Journal of Hydrometeorology*, **6**, 233–247.
- Pitman, A. and Coauthors, 1999: Key results and implications from phase 1(c) of the project for intercomparison of land-surface parameterization schemes. *Climate Dynamics*, **15**, 673–684.
- Qu, W. and Coauthors, 1998: Sensitivity of latent heat flux from PILPS land-surface schemes to perturbations of surface air temperature. *Journal of Atmospheric Sciences*, **55**, 1909–1927.
- Ren, D. and M. Xue, 2004: A revised force-restore model for land surface modeling. *Journal of Applied Meteorology*, **43**, 1768–1782.
- Schaap, M. G. and F. J. Leij, 1998: Database-related accuracy and uncertainty of pedotransfer functions. *Soil Science*, **163**, 765–779.
- Schlosser, C. and Coauthors, 2000: Simulations of a boreal grass-land hydrology at Valdai, Russia: PILPS phase 2(d). *Monthly Weather Review*, **128**, 301–321.
- Shao, Y. and A. Henderson-Sellers, 1996: Modeling soil moisture: A project for intercomparison of land surface parameterization schemes phase 2(b). *Journal of Geophysical Research*, **101**, 7227–7250.
- Vine, D. M. L., T. J. Jackson, C. T. Swift, M. Haken, and S. W. Bidwell, 2001: ESTAR Measurements during the Southern Great Plains experiment (SGP99). *IEEE Transactions on Geoscience And Remote Sensing*, **39**, 1680–1685.
- Xue, M., K. K. Droegemeier, and V. Wong, 2000: The advanced regional prediction system (ARPS): A multi-scale non-hydrostatic atmospheric simulation and prediction model. Part I: Model dynamics and verification. *Meteorology and Atmospheric Physics*, **75**, 161–193.
- Xue, M., K. K. Droegemeier, V. Wong, A. Shapiro, K. Brewster, F. Carr, D. Weber, Y. Liu, and D. Wang, 2001: The advanced regional prediction system (ARPS): A multi-scale non-hydrostatic atmospheric simulation and prediction tool. Part II: Model physics and applications. *Meteorology And Atmospheric Physics*, **76**, 143–165.
- Yeh, P.-F. and E. Eltahir, 2005: Representation of water table dynamics in a land-surface scheme. part i: Model development. *Journal of Climate*, **18**, 1861–1880.
- York, J. P., M. Person, W. J. Gutowski, and T. C. Winter, 2002: Putting aquifers into atmospheric simulation models: an example from the Mill Creek watershed, northeastern Kansas. *Advances in Water Resources*, **25**, 221–238.